Article:
Capetillo, A, Noakes, CJ and Sleigh, PA (2015) Computational fluid dynamics analysis to assess performance variability of in-duct UV-C systems. Science and Technology for the Built Environment, 21 (1). pp. 45-53. ISSN 2374-4731

https://doi.org/10.1080/10789669.2014.968512

CFD Analysis to Assess Performance Variability of In-Duct UV-C Systems

Azael Capetillo, Catherine J. Noakes*, P. Andrew Sleigh

Pathogen Control Engineering Institute, School of Civil Engineering, University of Leeds, Leeds, LS2 9JT, UK

**Corresponding author: C.J.Noakes@leeds.ac.uk*

ABSTRACT

UV-C is becoming a mainstream air sterilisation technology, and is marketed in the form of energy saving and infection reduction devices. An accurate rating of device performance is essential to ensure appropriate microbial reduction yet avoid wastage of energy due to over performance. This paper demonstrates the potential benefits from using computational fluid dynamics (CFD) to assess performance.

A CFD model was developed using discrete ordinate (DO) irradiation modeling and Lagrangian particle tracking to model airborne microorganisms. The study calculates UV dose received by airborne particles in an in-duct UV system based on published EPA experimental tests for single, four lamp and eight lamp devices. Whereas the EPA tests back calculated UV dose from measured microorganism inactivation data, the CFD model directly computes UV dose, then determines inactivation of microorganisms.

Microorganism inactivation values compared well between the CFD model and the EPA tests, but differences between UV dosages were found due to uncertainty in microorganism UV susceptibility data. The study highlighted the need for careful consideration of test microorganisms and a reliable data set of UV susceptibility values in air to assess performance. Evaluation of the dose distribution demonstrated the importance of creating an even UV field to minimize the risk of ineffective sterilization of some particles while not delivering excessive energy to others.

INTRODUCTION

Air cleaning technologies are used to control the indoor air quality by removing or inactivating contaminants in the environment. Such technologies may also have a role in energy efficiency by enabling recirculation of air and keeping HVAC equipment free of deposited particles and microbial growth which diminish airflow rates and affect heat transfer (Fisk et al., 2002). Fibrous mechanical filtration, which employs trapping and adsorption mechanisms (Sutherland, 2007), can be considered the most popular air cleaning technology. However filters that are capable of removing very small particles such as airborne microorganisms induce a large pressure drop in an HVAC system, increasing energy consumption (Fisk et al., 2002). In recent years interest has grown in the potential for photochemical air filters, such as UV-C irradiation, to supplement or replace fine particle filtration for microbial control. These devices have the capacity of destroying or decomposing microorganisms and potentially VOCs, and may have energy performance benefits over conventional filters (Blatt, 2006, Kowalski, 2009, Lee et al., 2009).

In-duct devices typically comprise one or more UV-C lamps mounted within the HVAC system to create a UV irradiation field inside an airflow duct. Microorganisms contained in the air passing through the UV field incur DNA damage proportional to the UV irradiance, time of exposure and species of microorganism; with sufficient exposure the damage may be lethal rendering microorganisms inactive. The technology has also shown reduction of bacteria concentration on surfaces after UV-C has been installed within a ventilation system (Taylor et al., 1995), leading to applications for reducing bio fouling of cooling coils and the potential for improving system energy efficiency (Blatt, 2006, Kowalski, 2009, Lee et al., 2009). With increasing application of in-duct UV-C systems, it is important to accurately quantify the technology's performance, and appropriate analysis and test mechanisms must be set in place. For an in-duct air system, the efficiency of UV-C sterilisation depends on many factors including UV irradiation intensity, dwell time of the microorganisms in the UV field within a duct or device, microorganism susceptibility to UV irradiation, air velocity, air temperature, and humidity, reflectivity of duct or device internal surfaces, velocity profile, air mixing and lamp position.

A number of studies have explored the influence of some these parameters through mathematical modeling. Kowalski (2009) predicted UV device performance with average irradiation fields determined using a view factor approximation, and Lau (2009) explored the effects of airflow velocity and temperature on lamp output. However these models assumed a fully mixed airflow and did not consider the 3D flow-UV field interaction that happens in a real case. Computational Fluid Dynamics (CFD) modeling can take this into account and has been successfully applied to UV water systems (Wright and Hargreaves, 2001) and upper-room UV (Gilkeson and Noakes, 2013). This same issue is also apparent in experimental assessment of UV device efficacy. The EPA tests series "Biological Inactivation Efficiency by HVAC In-Duct Ultraviolet Light Systems" (EPA 2006a, 2006b, 2006c) presents experimental data on UV inactivation and are a popular reference for the performance of UV in-duct sterilisation systems. However such tests only show mean performances and give little insight into the mechanisms for airflow and microorganism interaction with the UV field.

With the help of CFD analysis, hidden details of the performance of in-duct devices which cannot be shown on a biodosimetry test can be revealed. Through simulation of three EPA tests, this paper demonstrates the capabilities of CFD analysis for assessing in-duct UV air sterilization devices, highlighting the variability in performance due to flow patterns and the importance of UV susceptibility and decay model assumptions on biodosimetry test results.

EPA EXPERIMENTAL TESTS

The study compared CFD simulations to three EPA tests; EPA 600/R-06/050 which used a device containing a single 53 cm mercury lamp located perpendicular to the air flow, EPA 600/R-06/051 which compromises a device using four 53 cm long UV lamps located perpendicular to the airflow and evenly distributed over the height of the duct, and EPA 600/R-06/055 which uses a system of 8 UV lamps each 41.4 cm in length installed perpendicular to the airflow in two arrays of four lamps over the heignt of the duct. These tests are conducted on real devices and show increasingly complex lamp geometry for comparison between experimental results and CFD. The lamp and UV systems specifications for each test are listed in Table 1. The EPA experimental tests were conducted using two bacteria (*Bacillus atrophaeus* and *Serratia*

Marcescens) and one virus (MS2 Bacteriophage) aerosolized into an enclosed ducting ventilation test unit. The studies used bioaerosol samples taken before and after the UV device to quantify the efficacy of the UV sterilization system in terms of the fraction of microorganisms surviving. Full details of the experimental methods adopted by the EPA are given in the reports (EPA 2006a, 2006b, 2006c).

Table 1. EPA 600/R-06/050 test specifications.

Parameter	600/R-06/050	600/R-06/051	600/R-06/055
Number of lamps	1	4	8
Lamp power	58 Watts	25 Watts	60 Watts
Lamp UVC power	19 Watts	8.5 Watts	18 Watts
Total system power	58 Watts	100 Watts	480 Watts
Total system UV power	19 Watts	34 Watts	144 Watts
Lamp length	53.3 cm	53.82 cm	41 cm
Lamp diameter	1.9 cm T6	1.9 cm T6	1.9 cm T6
Duct	61 cm x 61 cm	61 cm x 61 cm	61 cm x 61 cm

In each case the average UV dose delivered by the UV device was calculated assuming a single stage decay model. As shown in equation 1, the microorganism survival fraction, S can be given by.

$$S = e^{-K.D} \qquad (1)$$

Here, k is the microorganism UV susceptibility expressed in $m^2.J^{-1}$ and D is the UV dose received by the microorganisms expressed in $J.m^{-2}$. From equation 1 we can calculate UV dose by rearranging to yield equation 2.

$$D = -\frac{\ln(S)}{k} \qquad (2)$$

Experimental results in the test reports were expressed in terms of microbiological inactivation or "kill" (1-survival), and a calculated mean UV dose was obtained with equation 2 using a microorganism susceptibility constant for *B. atrophaeus*. The reported inactivation and calculated UV dose are shown in Table 2. Kowalski (2009) later used the same inactivation rates to calculate a dose of 10 $J.m^{-2}$ for the EPA 600/R-06/050, 18 $J.m^{-2}$ for the EPA 600/R-06/051 and 73 $J.m^{-2}$ for the EPA 600/R-06/055; the reasons for the difference are discussed in the results section below along with the newly calculated UV dosages determined from the CFD analysis.

Table 2. EPA tests reported microbial inactivation.

Microorganism	600/R-06/050	600/R-06/051	600/R-06/055
S. Marcesens	99%	99.8%	99.9%
MS2	39%	46%	82%
B. atrophaeus	4%	0%	40%
EPA reported average UV dose J.m-2	2.47	2.95	31.80

COMPUTATIONAL FLUID DYNAMICS MODELLING

CFD models of the EPA tests described above were developed using Fluent (ANSYS v14.0). The geometry of the UV chamber was based on details reported by EPA, and consisted of a duct with a cross-sectional area of 0.61 x 0.61 m and a length of 1.83 m (Kowalski, 2009) as shown in Figure 1. A structured mesh containing 280,000 cells refined close to the lamps was defined using the ANSYS meshing module; the quality of this mesh is discussed in the results section below.

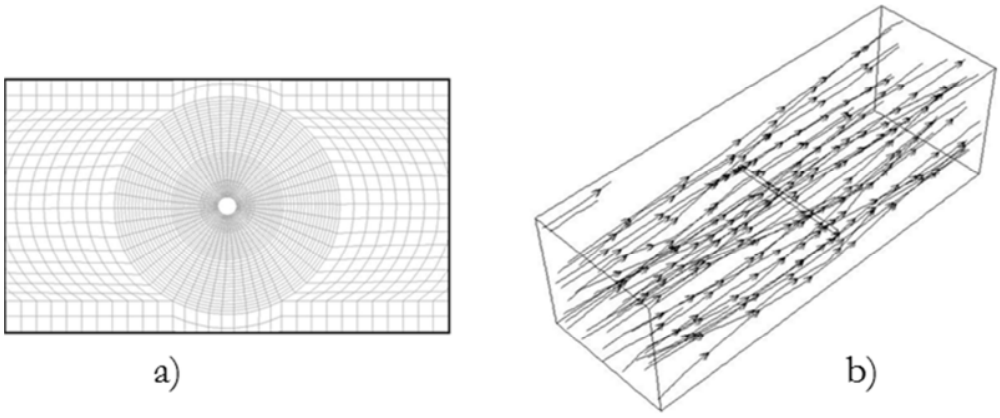

Figure 1 CFD modelgeometry for the single lamp case showing (a) an example mesh around the lamp and (b) modeled particle trajectories passing the lamp in the duct.

Mathematical modeling of the UV irradiation field in an air sterilisation reactor is essential for calculation of performance and further optimization. Irradiation models have been widely debated in literature, and yet a definitive model does not exist. A common drawback of analytical models is their inability to account for physical phenomena such as light absorption, emission or scattering, as in the case of the Inverse

Square model (Beggs, 2002), Point Source models (Bolton, 2000, Irazoqui et al., 1976) and Line Source model (Irazoqui et al., 1976). Physical models such as the Radiative Transfer Equation (RTE) (Cassano et al., 1995) represent propagation of radiation through a media, and states that as a beam of radiation travels it loses energy to absorption, gains energy by emission, and redistributes energy by scattering.. As expected, the more sophisticated the model is, the more difficult to solve. However with the use of CFD, complex models such as the RTE can be solved by the Discrete Ordinates (DO) method (Ho, 2009).

In this case, the ANSYS Fluent DO non-gray radiation model is applied, to solve the RTE (equation 3) for a finite number of discrete solid angles at a single wavelength λ, in this case 254 nm.

$$\nabla.(I_\lambda(\vec{r},\vec{s})\vec{s}) + (a_\lambda + \sigma_s)I_\lambda(\vec{r},\vec{s}) = a_\lambda n^2 I_{b\lambda} + \frac{\sigma_s}{4\pi}\int_0^{4\pi} I_\lambda(\vec{r},\vec{s}')\Phi(\vec{s}.\vec{s}')d\Omega' \quad (3)$$

Here:

$\vec{r}$ = position vector
$\vec{s}$ = direction vector
$\vec{s}'$ = scattering direction vector
s = path length
a_λ = absorption coefficient
n = refractive index
σ_s = scattering coefficient
$I_{b\lambda}$ = black body intensity
I_λ = radiation intensity, which depends on position ($\vec{r}$) and direction ($\vec{s}$)
λ = wavelength
Φ = phase function
Ω' = solid angle

By solving the RTE in a discretised manner it is possible to calculate the 3D irradiation profile around a UV lamp ($W.m^{-2}$). A comprehensive explaination of the DO model can be found in the work of Cassano et al. (1995). Within the Fluent DO model the material properties, the lamp output, and angular discretization parameters are defined by the user (ANSYS, 2009). The angular discretization is a key parameter as it defines the distribution of the irradiation within the numerical model (Pareek, 2004). Although the average irradiation in the domain area will remain the same, the distribution of the irradiation will vary depending on the mesh and two parameters, θ and ϕ, that define the discrete solid angles; the more angular divisions the more even the

the resulting irradiation field. In this case 10 divisions for both θ and ϕ were used as this gave a field distribution of acceptable quality for the mesh without excessive computational time.

The materials used for the simulation were air as fluid and aluminum as solid walls. All properties remained as standard, except for the absorption coefficient and refractive index of aluminum which were adjusted to fit the wavelength of sterilisation UV light (253.7 nm) with values of 1474900 m^{-1} and 0.19097 respectively (Polyanskiy, 2011). Reflection is an integral part of the RTE model, and is accounted by the internal emissivity of the material, basically a surface producing reflections acts as a source of radiation emitting power in relation with the material light absorption and the energy it receives. This extra irradiation is then added to the irradiation field within the system. Lamp output was based on the power and geometry stated in the EPA reports (Table 1). Flow was assumed to be steady and isothermal in all cases, with turbulence approximated through the k-epsilon model with standard wall functions. Boundary conditions were set as indicated in Table 3.

Table 3. CFD Model Boundary Conditions.

Zone	Property	600/R-06/050	600/R-06/051	600/R-06/055
Inlet	Velocity magnitude ($m.s^{-1}$)	2.5	2.5	2.5
	Turbulent intensity (%)	10	10	10
	Hydraulic diameter (m)	0.61	0.61	0.61
Walls	No slip	-	-	-
UV lamps	Direct irradiation ($W.m^{-2}$)	0	0	0
	Diffuse irradiation ($W.m^{-2}$)	597.2 per lamp	294.17 per lamp	494.36 per lamp

Second order discretization was applied and calculations were run for approximatly 3000 iterations. Once a converged flow field had been obtained, a Lagrangian particle model with Discrete Random Walk was used to simulate airborne microorganisms carried by the flow (King et al., 2013). Particles with physical characteristics of water liquid droplets and a diameter distribution ranging from $1x10^{-6}$ to $1x10^{-4}$ m were injected by surface at the inlet of the CFD models.

A user defined function adapted from Ho (2009) was used to determine the cumulative UV dose ($J.m^{-2}$) received by each particle as it passed through the UV field by a trapezoidal rule to approximate the integral

(equation 4).

$$UV\ dose = dT * \sum_{i=1}^{i=n} \frac{UV_i + UV_{i+1}}{2} \quad (4)$$

Here dT is a time interval, UV_i and UV_{i+1} are the UV irradiances in the computational cell at the beginning and end of the time step. Microorganism inactivation was calculated from the received dose at the end of the computational domain, using equation (1) with an appropriate microorganism susceptibility constant.

RESULTS AND DISCUSSION

Mesh independency tests were carried out for the single lamp (EPA 600/R-06/050) CFD model. The simulation was initially run for three different mesh sizes containing 100,000, 160,000 and 280,000 elements respectively. In each case the average UV dose at the end of the domain was calculated using the arithmetic mean of all the particle tracks. All three meshes yielded similar results, with values of average UV dose in the range 9.73 to 10.09 J.m^{-2} (Table 4). These results are consistent with each other and are also in good agreement with the dose of 10 J.m^{-2} calculated by Kowalski (2009) for these same EPA experimental tests using an analytical approach that did not take into consideration airflow patterns or particle trajectories. Although the behavior of the three mesh sizes are similar, the 280,000 mesh is able to better capture the subtleties of the dose distribution due to the greater number of particles tracked, and for this reasonsis used in further simulations. The other two models, EPA 600/R-06/051 and EPA 600/R-06/055, were simulated using the same element size as the 280,000 mesh for the EPA 600/R-06/050 CFD model.

Table 4. Calculated UV Dose for the Three mesh sizes for the EPA 600/R-06/050 CFD Models.

Model	Average Dose J/m^2	Average velocity (m/s)	Average pressure (Pa)	No. Particles
100 k mesh	10.09	2.499	0.19	6510
160 k mesh	10.08	2.500	0.20	9841
280 k mesh	9.73	2.499	0.21	14390
Kowalski (2009)	10	2.500	-	-

Influence of UV susceptibility for the single lamp model

All three EPA test reports measured microbiological kill rate of *B. atrophaeus, S. marcescens* and *MS2 bacteriophage*, then determined UV dose via back calculation based on the susceptilibity of *B. atrophaeus*. However the CFD model directly calculates UV dose from the trajectory of the simulated microorganism through the UV field, then determines inactivation. Both approaches depend on appropriate data for microorganism susceptibility. To compare the CFD results directly to the EPA tests each microorganism was independently considered in the single lamp model with published UV susceptibility data.

The UV susceptibility of *S. marcescens* in air has been extensively tested. Fletcher et al. (2003) shows comprehensive survival data for *S. marcescens* under various UV doses at two different humidity levels that suggests the microorganism can be represented using a single stage decay model. Their calculated susceptibility constant of 0.939 $m^2.J^{-1}$ compares well to the value of 0.92 $m^2.J^{-1}$ given by Lai et al (2004), although both are higher than the value of 0.445 $m^2.J^{-1}$ reported in Sharp (1940). As shown in Table 5, calculated inactivation for *S. marcescens* from the EPA 600/R-06/050 CFD model at the average dose of 9.73 $J.m^{-2}$ are in good agreement to the EPA measured values for these three published *k* factors for relative humidities of up to 70%.

Table 5. EPA 600/R-06/050 CFD Calculated Performance Against *Test results*

Reference values	Microorganism	RH %	CFD Dose $J.m^{-2}$	Shoulder n value	K $m^2.J^{-1}$	EPA Test inactivation	CFD calculated inactivation
Fletcher 2003	*S. marcescens*	48	9.73	-	0.939	99%	99.98%
Sharp 1940		Low		-	0.445		98.65%
Lai 2004		68		-	0.92		99.98%
Average		-		-	*0.662*		*99.46%*
Walker 2007	MS2 Bacteriophage	32-50	9.73	-	0.038	39%	30.78%
Walker 2007		74-85		-	0.048		37.16%
Average		-		-	*0.043*		*34.05%*
EPA 2006	*B. subtillis* (*B. atrophaeus*)	-	9.73	-	0.016	4%	15.20%
VanOsdell 2002				-	0.02		17.34%
Ke et al. 2009		50-60		3	0.017		0.62%
Ke et al. 2009		70-83		2	0.014		1.71%
Average		-		-	-		*8.72%*

For the case of MS2 bacteriophage, Walker et al. (2007) reported susceptibility values of k=0.038 $m^2.J^{-1}$ for 32-50% relative humidity and k=0.048 $m^2.J^{-1}$ for 74-82% relative humidity. Using these values, and again assuming the single stage decay model (equation 1), the inactivation calculated from the CFD model again compares well to the results of the EPA 600/R-06/050 experimental test, as shown inTable 5.

Bacillus atrophaeus is a reclassification of certain strains of *Bacillus subtillis* (Fritze and Pukall, 2001, Nakamura, 1989). The susceptibility value used by EPA (2006a) is k=0.016 $m^2.J^{-1}$ and assumed a single stage decay. The RTI study by VanOsdell and Foarde(2002) reported the susceptibility of *B. subtilis* spores to be 0.02 $m^2.J^{-1}$. However studies have shown that *B. subtilis* spores do not follow a first order decay model and are better represented with a shoulder (n) in the decay model (Kowalski, 2009, Nicholson and Galeano, 2003). Ke et al. (2009) reported the susceptibility value of *B. subtilis* spores to be 0.017 $m^2.J^{-1}$ with a shoulder of n=3 for relative humidity levels of 50 to 60% and 0.014 $m^2.J^{-1}$ with a shoulder of n=2 for relative humidity levels of 70 to 83%.

It can be seen from Table 5 that there is considerable variation in the calculated inactivation of *B. atrophaeus* from the CFD model UV dose depending on the susceptibility constant and and whether single stage or shoulder decay assumptions are used. This is of paramount importance if measured inactivation rates are used to calculate by regression the UV dose, and explains why the reported UV dose calculated from the EPA tests (Table 2) is lower than that determined here or by Kowalski (2009). The EPA test 600/R-06/050 rated the performance of the single lamp UV system to be 2.47 $J.m^{-2}$ (247 $\mu W.S.cm^{-2}$); obtained by regression of the kill rate of *B. atrophaeus* in single stage decay at the susceptibility value of 0.016 $m^2.J^{-1}$ (EPA, 2006). If such a UV dose value is used to calculate the inactivation of the other tested microorganisms, *S. marcescens* and MS2 Bacteriophage, using the average susceptibility constants as given in Table 5, we would obtain the results as shown in Table 6.

Table 6. Average Calculated Kill Rate at 2.47 $J.m^{-2}$ Dose

Microorganism	Dose $J.m^{-2}$	Reference	Calculated inactivation	EPA measured inactivation
B. atrophaeus	2.47	Average	2.20 %	4%
S. marcescens		Average	90.16%	99%
MS2 Bacteriophage		Average	10.07%	39%

The UV dose stated in the EPA report is more than three times lower than that calculated from the CFD model, and as illustrated by the calculation in Table 6 is clearly an underestimation. The UV dose delivered by an enclosed UV system working under normal constant operation should remain constant as it is function of the physical and irradiation parameters of the system only. Therefore when calculating the UV dose of a system by regression of biodosimetry test results, the calculated dose of the system should remain constant independent of the microorganism used; if it is different, then it is an indication that the microorganism decay model used for the calculation is wrong.

UV dose distribution within a duct

CFD analysis can help to visualize important data which otherwise would be impossible to capture on a biodosimetry test. While the average UV dose for the single lamp model is calculated at 9.73 $J.m^{-2}$ the CFD model is able to show the variation of the dose within the system. Figure 2 shows the dose distribution received by particles at the end of the duct. From this distribution it can be seen that the mode UV dosage is 6.5 $J.m^{-2}$, considerably lower than the average. The average dose appears to be increased by a small number of particles gaining a very high dose, while a large population (53% of particles) receive less than the average dose.

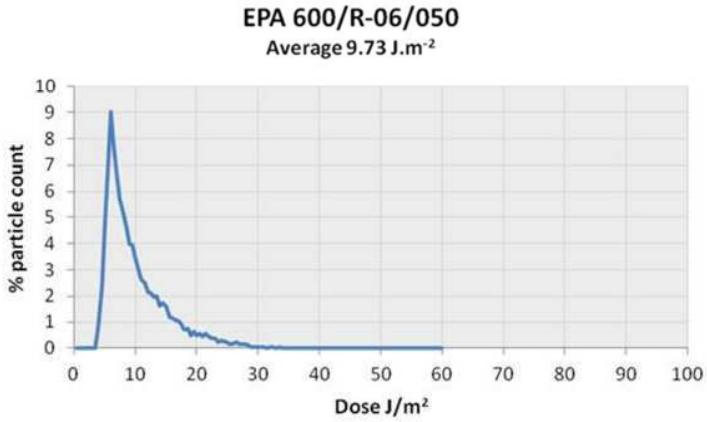

Figure 2 Dose distributions by particle track at the end of the duct for the single lamp case.

In reference to Figure 2, the ideal design would deliver a single sharp peak with all particles receiving the required UV dose; particles receiving less are underexposed and those receiving more UV dose than necessary would be translated as waste of resources. Figure 3 shows the distribution of UV dose at the end of the duct in relation to the duct cross-section and lamp location. Each point on the plots represents one of the simulated particle locations. The results indicate that duct corners have the lowest average irradiation values, with particles here receiving the lowest dose (a), while those that pass close to the lamp have generally have higher than the average dose (b). This highlights the impact of lamp location and configuration, and the need to improve dose distribution while reducing energy consumption.

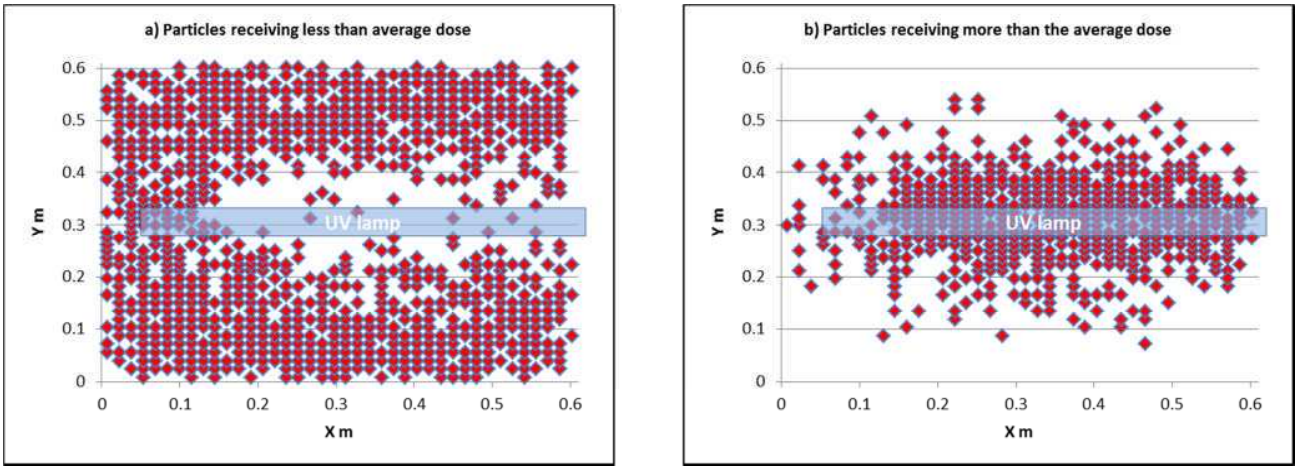

Figure 3 Cross section of the duct outlet showing the lamp position and (a) particles receiving less than the averaged dose <9.7 J.m^{-2}, (b) particles receiving the average dose or more >9.7 J.m^{-2}.

Influence of lamp configuration

Following the single lamp simulations, further CFD simulations were carried out to evaluate the four (EPA 600/R-0/051) and eight (EPA 600/R-06/055) lamp cases, which contain a more complex UV lamp geometry shown in Figure 4.

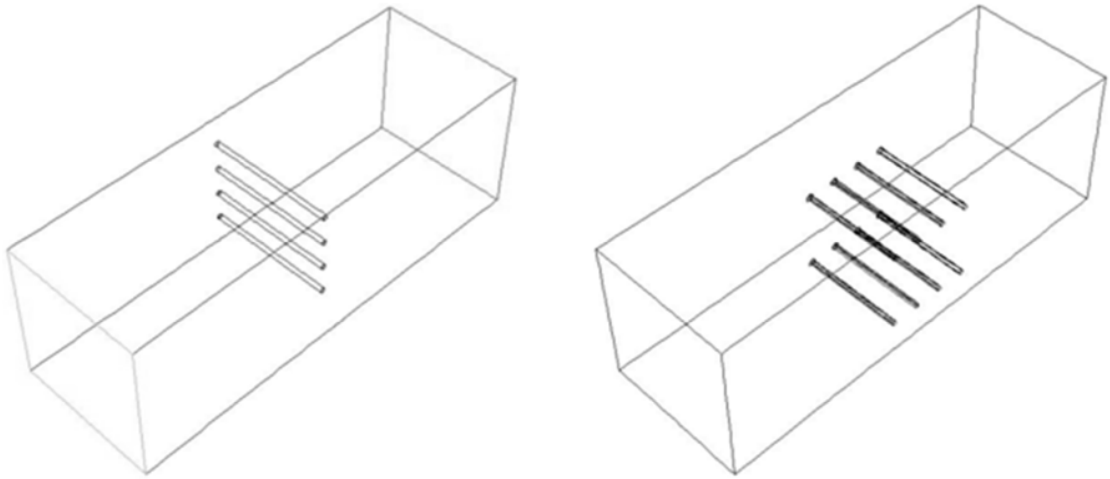

Figure 4 Geometry model for the 4 lamp (EPA 600/R-06/051) and 8 lamp (EPA 600/R-06/055) cases.

As shown in Table 7 the inactivation calculated from the CFD models using the average susceptibility values in Table 4 are generally similar to the reported microorganism inactivation in the EPA tests. However the UV dose calculated from the CFD simulations is again higher than stated in the EPA reports. This isfor the same reasons as outlined above for the single lamp case. In the four lamp case the EPA 600/R-06/051 test reported a UV dose of 2.95 $J.m^{-2}$ (EPA, 2006b) while the CFD calculated dose is 15.82 $J.m^{-2}$, and in the eight lamp case the EPA 600/R-06/055 test reported 39.84 $J.m^{-2}$ while the CFD calculated dose is 58.23 $J.m^{-2}$ (EPA, 2006c).

It can be seen in Table 7 that the EPA 600/R-06/051 four lamp test reported a 0.00% kill rate on *B. atrophaeus*, while the CFD model predicts 13.68%. It is thought that this value of 0.00% is an error in the experimental data, as a higher UV power (34 W) than the single lamp model should result in a higher kill rate than reported in EPA 600/R-06/050 (18 W). It is also worth commenting on the results for *S. marcescens*. This shows very close comparison between CFD and experiments for all three lamp configurations. However, the susceptibility constant, *k*, is so high that any UV dose over 10 $J.m^{-2}$ would show a 99.99% kill rate. It is therefore it is not a good reference microrganism to conduct UV dose calculations or experimental assessments for duct mounted installations.

Table 7. CFD Calculated Performance Against *Test results*

Reference values	Microorganism	600/R-06/051		600/R06/055	
		CFD calculated %Kill rate	EPA reported %Kill rate	CFD calculated %Kill rate	EPA reported %Kill rate
Average	*S. marcescens*	99.99	99.99	100.00	99.9
Average	MS2 Bacteriophage	49.35	46.00	91.82	82.00
Average	*B. subtillis* (*B. atrophaeus*)	13.68	0.00	46.32	40.00

As with the single lamp case, the CFD analysis of these multi-lamp devices also shows how dose distribution changes according to lamp geometry and UV power. The case with four lamps evenly distributed over the height of the duct (Figure 5 (a)) shows a double peaked distribution, with the mode closer to the average UV dose of the system than in the single lamp case. The eight lamp model shows a wider dose distribution, yet the peak is again closer to the system average UV dose.

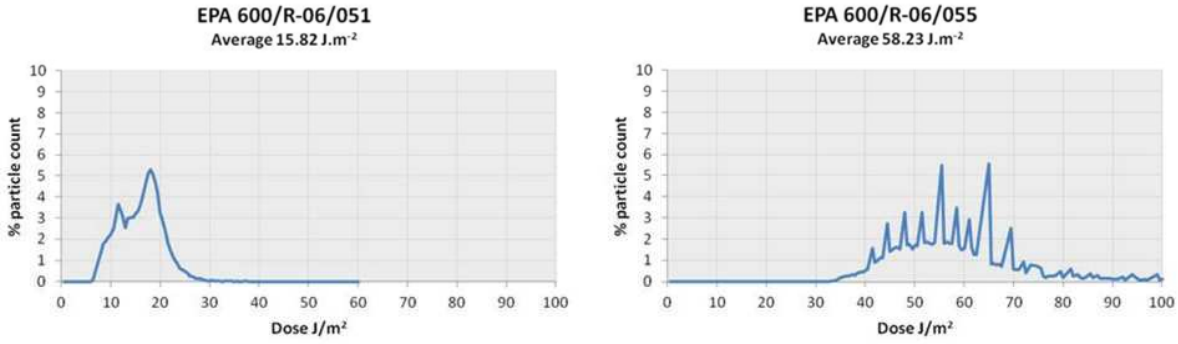

Figure 5 Dose distributions for (a) EPA 600/R-06/051 and (b) EPA 600/R-06/055.

Figure 6 shows the location of particles that received the average UV dose of the system or more for the four (a) and eight (b) lamp models. It can be seen again that there are few particles at the corners receiving sufficient UV dose, however in both cases there is greater coverage than the single lamp case indicating a more even distribution.

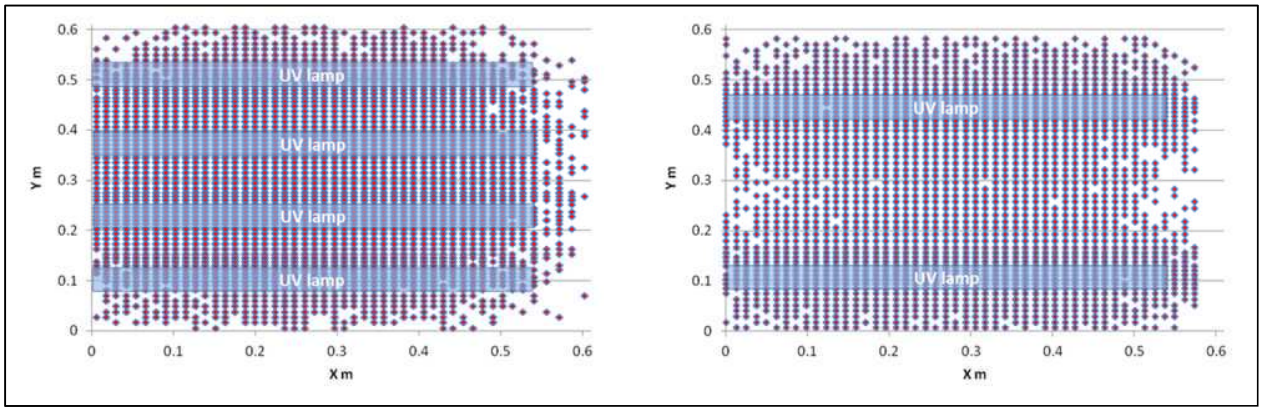

Figure 6 Cross section of the duct outlet showing the lamp position and particles receiving the average dose or more (a) 4 lamp case (EPA 600/R-06/051) (b) 8 lamp case (EPA 600/R-06/055).

Comparing all three cases indictates that the more even the UV dose distribution, the more efficient the system is. Results for the single lamp system show that 3.15% of particles received half the average dose of the system or less, while 6.2% received double the average dose of the system. These values change when the dose is more closely distributed towards the average. In the four lamp design 1.73% of particles received less than half the average dose and only 0.4% of particles received double than the average dose and for the 8 lamp system there were no particles receiving less than half the average dose and only 0.9% received double the average dose. This indicates that the energy input into the device is being better used, with the more even distribution resulting in substantially less under and over performance.

Model limitations

While the CFD simulation results are in good agreement with the experimental results, it is important to consider the limitations of the model. The model assumes isothermal flow, however in reality the lamp will act as a heat source and the incoming air into the system may range from 0^{o}C or less to over 35 ^{o}C depending on the local climate, whether it is outdoor or indoor air and whether it has had any pre-conditioning prior to UV irradiation. It is likely that the flow pattern in a ventilation duct will be largely straight and dominated by the velocity provided by the fan. The presence of the lamp heat source may increase the mixing in the duct slightly, which may be beneficial from a UV disinfection perspective. Where there is a large temperature

gradient between the air and the lamp and at low flow rates, buoyancy effects may influence the flow field and may need to be included in models. Similarly, the influence of lamp mounting arrangements have not been considered, which may also promote mixing of the airflow in the system.

CONCLUSIONS AND FUTURE WORK

This study compares CFD modeling of three in-duct UV systems with published experimental data, and demonstrates that CFD models are a viable method of predicting performance and supporting system design. Discrete Ordinate UV irradiance models applied in a CFD modelappear to be a reliable technique for the calculation of the UV field, UV dose and microorganism inactivation within in-duct UV sterilization systems. Good comparison is seen between CFD calculated inactivation, EPA (2006a, 2006b, 2006c) test results, and previously published average UV dose calculations (Kowalski, 2009).

The results highlight important considerations in selecting appropriate test microorganisms for performance assessments. *B. subtilis* and *B. atrophaeus* present a shoulder on their decay curve. The results show that not accounting for such a shoulder when calculating UV dose by regression from microbiological tests may result in an under calculation of the UV system dosage. The results also indicate that *S. marcescens* is not a good reference microorganism for the calculation of a system UV dosage as it has a high susceptibility to UV and any dose over 10 $J.m^{-2}$ will result in kill rates of 99.99% regardless of system design.

The results also show the limitations of current UV susceptibility data in the literature. While there are a good number of studies that report susceptibility data, there is a considerable amount of variability between studies which depends on test conditions and the particular strain of a microorganism species. A more comprehensive database of UV susceptibility of microorganisms that includes the full spectrum of the microorganism decay is required for accurate calculation of the UV power demands for the sterilization of air. This is the case for performance assessment through modeling or experimental approaches.

System design and the method of evaluation are shown to have a significant effect on the energy efficiency and sterilization efficacy of a UV installation. Calculating UV dose by regression from biodosimetry tests using the wrong microorganism decay model or incorrect UV susceptibility values will result in miscalculation of UV dose. This in turn can lead to underpowered systems in which the sterilization efficiency

would be compromised or overpowered UV systems resulting in a waste of energy and excessive capital and maintenance costs. Furthermore the average dose delivered by a system may be a poor representation of its performance. In the single lamp case average data compares well between experiments and CFD models yet the CFD analysis showed that more than half particles received less than the average calculated dose and 6.2% received over double the average dose. This indicates a poor design with both under performance and excess energy use apparent within the same device. CFD analysis is capable of identifying this variability in dose distribution that otherwise would be impossible to identify by a biodosimetry test. Initial simulations with four and eight lamp configurations show the benefit of positioning lamps to create a more even UV irradiance field and hence UV dose in the system. However it is likely that neither of these are optimal solutions. Ongoing studies are focusing on lamp position optimisation to enable the most effective UV sterilization and the best use of the energy input into the system. This includes comparison of lamps positioned parallel or perpendicular to the airflow, and assessment of lamps located in staggered as well as inline arrangements within the duct.

ACKNOWLEDGEMENTS

This work was carried out as part of a PhD studentship funded by Conacyt (Mexico).

REFERENCES

ANSYS, I. 2009. *5.3.6 Discrete Ordinates (DO) Radiation Model Theory* [Online]. Available: https://www.sharcnet.ca/Software/Fluent12/html/th/node115.htm.

BEGGS, C. B. 2002. A Quantitative Method for Evaluating the Photoreactivation of Ultraviolet Damaged Microorganisms. *Photochemistry and Photobiological Science,* 1**,** 8.

BLATT, M. H. 2006. Avanced HVAC Systems for Improving Indoor Environmental Quality and Energy Performance of California K-12 Schools; Applications Guide for Off-the-Shelf Equipment for UVC Use. California Energy Commission.

BOLTON, J. R. 2000. Calculation of Ultraviolet Fluence Rate Distribution in an Annular Reactor: Significance of Refraction and Reflection. *Wat. Res.,* 34**,** 10.

CASSANO, A. E., MARTIN, C. A., BRANDI, R. J. & ALFANO, O. M. 1995. Photoreactor Analysis and Design: Fundamentals and Applications. *Ind. Eng. Chem. Res,* 34**,** 47.

EPA 2006a. EPA 600/R-06/050. Technology Evaluation Report. Biological Innactivation Efficiency by HVAC In-Duct Ultraviolet Light Systems. Dust Free Bio-Fighter 4Xtreme, model 21.

EPA 2006b. EPA 600/R-06/051 Biological Inactivation Efficiency by HVAC In-Duct Ultraviolet Light Systems Atlantic Ultraviolet Corporation Aerologic Model AD24-4. EPA.

EPA 2006c. EPA 600/R-06/055 Biological Innactivation Efficiency by HVAC In-Duct Ultraviolet Light Systems. Lumalier ADPL-60-8. EPA.

FISK, W. J., FAULKNER, D., PALONEN, J. & SEPPANEN, O. 2002. Performance and Cost of Particle Air Filtration Technologies. *Indoor air,* 12**,** 12.

FLETCHER, L. A., NOAKES, C. J., BEGGS, C. B., SLEIGH, P. A. & KERR, K. G. 2003. The Ultraviolet Susceptibility of Aerolised Microorganisms and the Role of Photoreactivation. *Second international congress of the IUVA.* Vienna.

FRITZE, D. & PUKALL, R. 2001. Reclassification of Bioindicator Strains Bacillus subtilis DSM 675 and Bacillus subtilis DSM 2277 as Bacillus atrophaeus. *International Journal of Systematic and Evolutionary Microbiology,* 51**,** 35-37.

GILKESON, C. A. & NOAKES, C. J. 2013. Applications of CFD Simulation to Predicting Upper-room UVGI. *Photochemistry and Photobiological*.

HO, C. K. 2009. Radiation Dose Modeling in Fluent. WEF Disinfection 2009 Workshop: Modeling UV Disinfection using CFD: Sandia National Laboratories.

IRAZOQUI, H. A., CERDA, J. & CASSANO, A. E. 1976. The Radiation Field for the Point and Line Source Approximations and the Three-dimensional Source Models: Applications to Photoreactions. *The Chemical Engineering Journal,* 11**,** 11.

KE, Q. S., CRAIK, S. A., EL-DIN, M. G. & BOLTON, J. R. 2009. Development of a Protocol for the Determination of the Ultraviolet Sensitivity of Microorganisms Suspended in air. *Aerosol Science and Technology,* 43**,** 6.

KING, M. F., NOAKES, C. J., SLEIGH, P. A. & CAMARGO-VALERO, M. 2013. Bioaerosol Deposition in Single and Two-bed Hospital Rooms: A Numerical and Experimental Study. *Building and Environment,* 59**,** 11.

KOWALSKI, W. 2009. *Ultraviolet Germicidal Irradiation Handbook*, Springer.

LAI, K., BURGE, H. A. & FIRST, M. 2004. Size and UV germicidal irradiation susceptibility of Serratia marcescens when aerosolized from different suspending media. *Applied and Environmental Microbiology,* 70**,** 8.

LAU, J. 2009. *Lamp and In-Duct Device Modelling For UVGI Systems Performance Prediction.* Doctor of Philosophy, The Pennsylvania State University.

LEE, B., BAHNFLETH, W. & AUER, K. Life-Cycle Cost Simulation of In-Duct Ultraviolet Germicidal Irradiation Systems. Proceedings of Building Simulation, 2009.

NAKAMURA, L. K. 1989. Taxonomic Relationship of Black-Pigmented Bacillus subtilis Strains and a Proposal for Bacillus atrophaeus sp. nov. *international journal of systematic Bacteriology,* 39**,** 295-300.

NICHOLSON, W. L. & GALEANO, B. 2003. UV Resistance of Bacillus anthracis spores Revisited: Validation of Bacillus spores as UV Surrogates for Spores of B. anthracis Sterne. *Applied and Environmental Microbiology,* 69**,** 4.

PAREEK, V.K., Light Intensity Distribution in a Phototcatalytics Reactor Using Finite Volume. AIChE Journal, 2004. 50(6): p. 16.

POLYANSKIY, M. 2011. *Refractive Index Database* [Online]. Available: http://refractiveindex.info [Accessed March 05 2012].

SHARP, G. 1940. The effects of ultraviolet light on bacteria suspended in air. *Journal of Bacteriology,* 38**,** 535-547.

SUTHERLAND, K. 2007. *Filters and Filtration Handbook*, Elsevier Science.

TAYLOR, G. J. S., BANNISTER, G. C. & LEEMING, J. P. 1995. Wound Disinfection With Ultraviolet Radiation. *Journal of hospital infection,* 30**,** 9.

VANOSDELL, D. & FOARDE, K. 2002. Defining the Effectiveness of UV lamps Installed in Circulating Air Ductwork. Arlington, VA: Air-Conditioning and Refrigeration Technology Institute (ARTI).

WALKER, C. & KO, G. 2007. Effect of Ultraviolet Germicidal Irradiation on Viral Aerosols. *Environ Sci Technol,* 41**,** 16.

WRIGHT, N. G. & HARGREAVES, D. M. 2001. The Use of CFD in the Evaluation of UV Treatment Systems. *Journal of Hydrinformatics,* 3**,** 59-70.